Calibration of Free-Space Radiometric Partial Discharge Measurements

Adel A. Jaber, Pavlos I. Lazaridis, Mohammad Moradzadeh, Ian A. Glover
University of Huddersfield,
Department of Engineering and Technology
Huddersfield HD1 3DH, UK

Zaharias D. Zaharis
Aristotle University of Thessaloniki
Department of Electrical and Computer Engineering
GR-54124 Thessaloniki, Greece

Maria F.Q. Vieira
Universidade Federal de Campina Grande
Department of Electrical and Engineering
58429-900 Campina Grande, PB, Brazil

Martin D. Judd
High-Frequency Diagnostics and Engineering Ltd
Glasgow G3 7JT, UK

and **Robert C. Atkinson**
University of Strathclyde
Glasgow G1 1XW, UK

ABSTRACT

The present study addresses the calibration of four types of partial discharge (PD) emulators used in the development of a PD Wireless Sensor Network (WSN). Three PD emulators have been constructed: a floating-electrode emulator, and two internal PD emulators. Both DC and AC high-voltage power supplies are used to initiate PD, which is measured using concurrent free-space radiometry (FSR) and a galvanic contact method based on the IEC 60270 standard. The emulators have been measured and simulated, and a good agreement has been found for the radiated fields. A new method of estimating the absolute PD activity level from radiometric measurements is proposed.

Index Terms — **Biconical antenna, FSR measurement, galvanic contact measurement, partial discharge, PD emulator calibration, PD intensity measurement.**

1 INTRODUCTION

ELECTRICITY supply organizations around the world are facing growing energy demand and an ageing transmission and distribution infrastructure. The cost of replacing infrastructure is high and careful management of existing plants is therefore required to prolong their use by minimizing the risk of failure. To facilitate efficient and reliable operation, continuous condition monitoring of the electrical equipment within substations is required [1].

A major problem in high-voltage (HV) power systems is degradation and breakdown of insulation. Statistics indicate that most HV equipment failures occur due to insulation breakdown [2]. Figure 1 shows the percentage of failures caused by insulation breakdown for a range of equipment categories [3 - 8].

Measurement of partial discharge (PD) is a useful way to identify incipient insulation faults. It provides the ability to monitor the progress of insulation deterioration resulting thus in informed decisions about when intervention is necessary. PD measurement has already been used to diagnose substation insulation faults, and predict imminent equipment failures with consequent reduction of system outage [9]. Partial discharge can be monitored by using optical, chemical, acoustic or electrical

Manuscript received on 27 March 2017, in final form 19 June 2017, accepted 20 June 2017. Corresponding author: Adel A. Jaber.

DOI: 10.1109/TDEI.2017.006730

methods. Traditional electrical PD measurements can be divided into galvanic contact and near-field coupling methods. The former is mostly used in an off-load test environment (often for acceptance testing of equipment), while the latter are mostly used in an on-load (operational) environment. Galvanic contact measurement, performed in accordance with the IEC 60270 standard, is generally accepted to provide the most accurate method of PD measurement and therefore is often used as a reference. Near-field coupling typically uses high-frequency current transformers (HFCTs) and/or transient earth voltage (TEV) sensors to collect PD data.

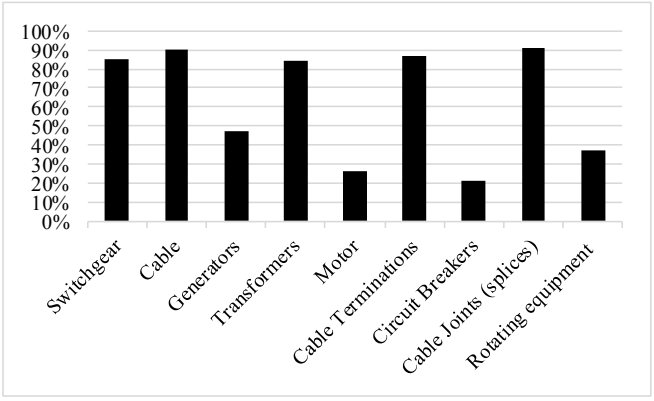

Figure 1. Proportion of failures due to insulation breakdown in different categories of HV plant. (compiled from [3 – 8]).

This requires a sensor to be physically attached to a particular plant item. The close coupling between the PD source and the wideband sensor (especially in the case of HFCTs) means that much of the information in and character of the PD signal is preserved; in particular, its apparent charge and signal spectrum. Valuable diagnostic content about the nature of the PD process resides in these characteristics. The energy spectrum, for example, can distinguish less damaging corona from more damaging internal PD due to insulation voids. The apparent charge, which is a measure of PD absolute intensity, can indicate the degree to which a PD process has advanced. This in turn may allow an early incipient insulation fault that does not require immediate attention to be distinguished from late-stage severe PD indicative of imminent plant failure.

The more recent free-space radiometric (FSR) method of PD measurement uses an antenna to receive signals radiated by the transient PD pulses. The precise relationship between the FSR signal at the receiving antenna terminals and the PD current pulse may be complicated [10]. There is, in addition, the possibility of further spectral distortion due to the frequency response of the radio propagation channel.

The application of FSR methods to measure the absolute PD intensity (i.e., apparent charge) has been considered to be difficult, if not impossible. This is because the received signal amplitude depends on several factors, which are unknown to a greater or lesser extent [12]. These unknown factors, in order of increasing difficulty to establish, are: (i) the path loss between radiating structure and receiving antenna, (ii) the polarization of the radiated field in the direction of the receiving antenna, (iii) the gain of the radiating structure in the direction of the receiving antenna, and (iv) the radiated power [1].

This paper has the following two objectives:

i. To compare the frequency spectrum of radiated PD signals with the spectrum measured by using the electrical galvanic contact method (the authors regard the latter as the measurement method most likely to preserve diagnostic information).

ii. To establish the plausibility of estimating effective radiated power (ERP) as an alternative measure of absolute PD intensity to apparent charge.

Figure 2 shows a PD measurement circuit similar to that specified in the IEC 60270 standard [13]. It comprises a coupling capacitor C_k, a test object C_a, a coupling device *CD* (with input impedance Z_{mi}), a coaxial cable *CC* and a measuring instrument *MI* [13]. The circuit measures the PD current pulse flowing through C_a. When a discharge occurs, the voltage across C_a decreases momentarily due to the voltage drop across the HV source impedance (Z in Figure 2) and this is compensated by charge flowing into C_a from C_k. As a result, a current pulse $i(t)$ of short duration (typically nanoseconds) flows through the measurement circuit and a voltage pulse $v_0(t)$ is generated across the *CD*, which is then detected by the *MI*. The apparent charge mentioned above is the integral of $i(t)$ and is typically of the order of picocoulombs. It is related to, but not exactly the same as, the charge transferred by the partial discharge event inside C_a [13].

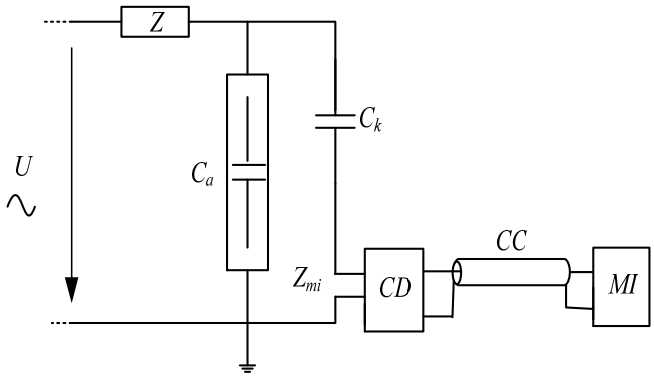

Figure 2. IEC 60270 PD measurement.

The apparent charge is assessed using the galvanic contact measurement illustrated in Figure 3. A short-duration current pulse representing a known charge q_0 is injected into the test object. The response of the *MI* can then be related to this known charge. The calibrator comprises a generator *G* generating step voltage pulses of amplitude V_0 in series with a high-accuracy capacitor C_0. If the voltage V_0 is precisely known, repeatable pulses equivalent to a charge $Q_{cal} = V_0 \times C_0$ are injected into the test device [14]. This procedure of measurement does not comply rigorously with the IEC60270 standard but the configuration of the measurement is similar.

The FSR measurement is illustrated in Figure 4. The antenna is a broadband biconical dipole and the digital sampling scope has an analogue measurement bandwidth of 4 GHz.

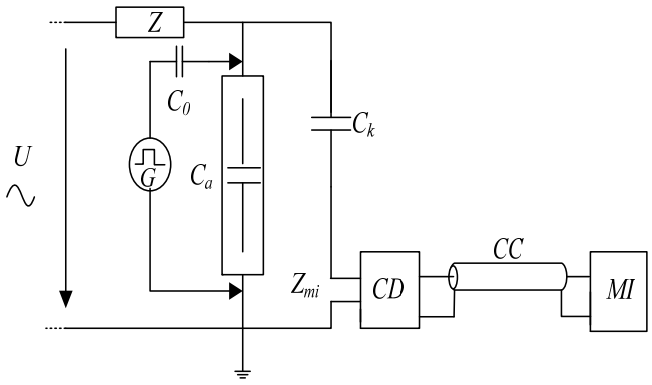

Figure 3. PD measurement calibration.

The four PD sources used to compare the FSR and galvanic contact signals are a floating electrode emulator, an acrylic tube internal emulator, an acrylic tube internal emulator filled with transformer oil, and an epoxy dielectric internal emulator. The floating electrode emulator is emulating GIS (Gas-Insulated Switchgear) defect induced PD, while the internal emulators are emulating power transformer defect induced PD. The measurements were carried out in a laboratory environment.

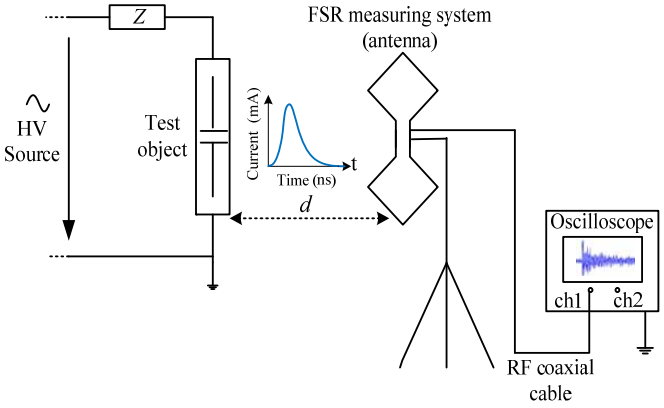

Figure 4. Free-space radiometric PD measurement.

The main body of the paper is divided into four sections. Section II describes the method and instrumentation used for the measurements. Section III presents the measurement results. Finally, section IV draws the conclusions.

2 EXPERIMENTAL APPARATUS FOR PD MEASUREMENT

The apparatus used to obtain concurrent galvanic contact and FSR measurements for the same PD event is shown in Figure 5 [15]. The experiment setup has been used for all four PD emulators.

PD is generated by applying high voltage to the artificial PD sources. The radiometric measurements are performed by using a biconical antenna connected to a 4 GHz, 20 GSa/s, digital sampling oscilloscope (DSO) [16].

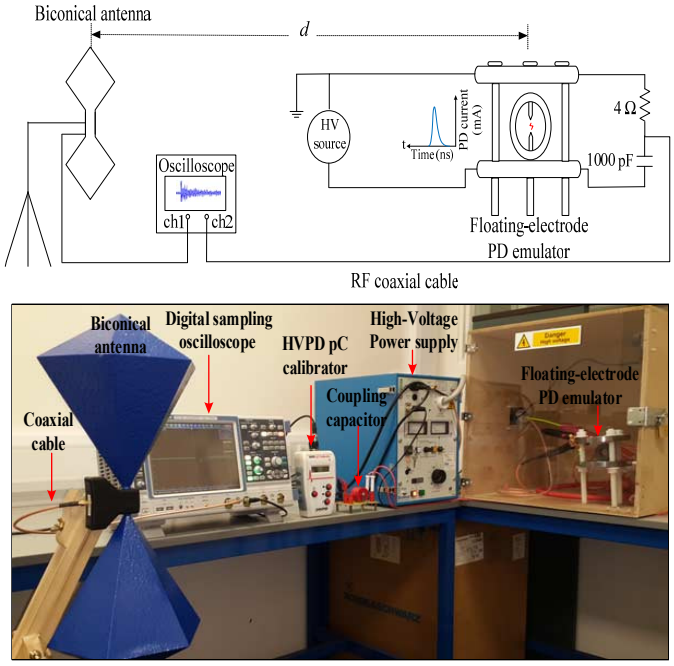

Figure 5. PD measurement apparatus.

The antenna frequency range is 20 MHz to 1 GHz, and its nominal input impedance is 50 Ohms. The antenna dimensions are 540 mm × 225 mm × 225 mm. As shown in Figure 6, the antenna factor measured by the manufacturer is between 17 dB/m and 25 dB/m for the frequency band of interest to this experiment, i.e., 50-470 MHz. The ERP is calculated by assuming free-space propagation and by using the values of the antenna factor provided by the manufacturer. The voltage rating of the galvanic contact coupling capacitor is 40 kV. The coupling capacitor protects the PD detector from high voltage and passes only the transient PD signal.

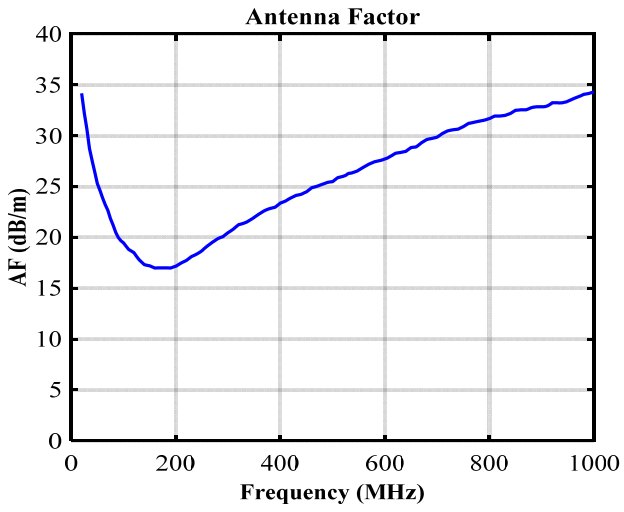

Figure 6. Biconical antenna factor vs. frequency.

The cage surrounding the emulators is made of wood and fiberglass so that it does not block electromagnetic radiation. The floating electrode PD emulator is shown in Figure 7. The

output of the HV power source is connected to the lower electrode and the upper electrode is connected to earth. When the electric field is sufficiently large, corona discharge originates from the floating electrode [17, 18].

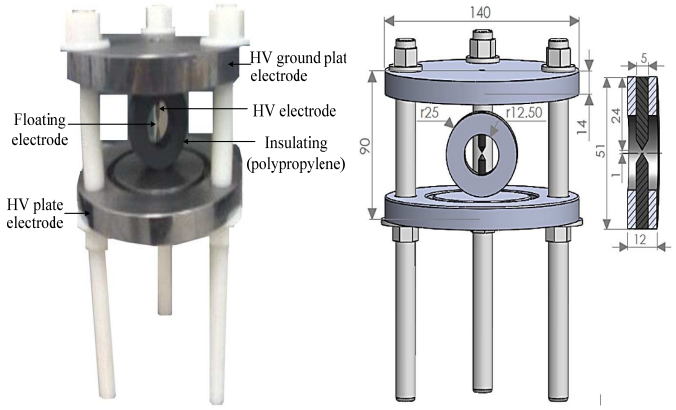

Figure 7. Floating electrode PD emulator (dimensions in mm) [18].

The acrylic tube PD emulator is shown in Figure 8. The electrodes are smaller than those in the floating electrode emulator. The edges of the electrodes have a circular profile to reduce the resulting corona, which usually occurs from sharp edges. The insulation comprises three circular plates made by perspex and being compressed between the two electrodes to form a composite disc. The thickness of each plate is 1.5 mm. The insulation defect is created by drilling a hole (1 mm in diameter) in the middle plate. The electrodes and the insulating disc are enclosed in an acrylic cylinder, which may be filled with transformer oil to avoid discharge from the disc edges [18, 19].

The epoxy dielectric internal PD emulator is shown in Figure 9. The insulation comprises three epoxy plates. A cavity is created by a 1 mm diameter hole drilled in the middle plate. The thickness of the three-plate composite disc is 2.4 mm. The HV electrode is made from stainless steel with a well-rounded edge to avoid surface discharge from regions of elevated field strength [18, 20].

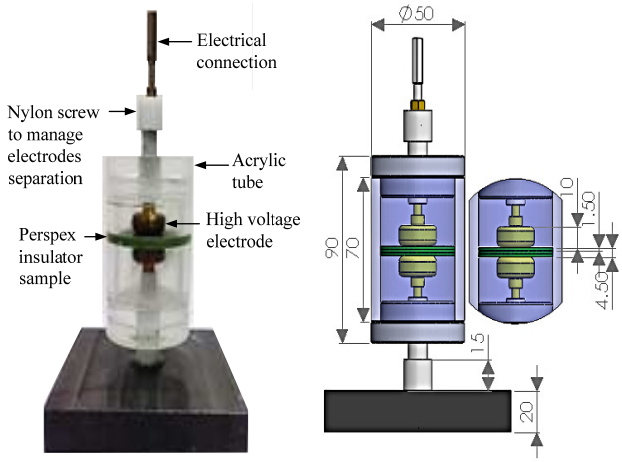

Figure 8. Acrylic tube PD emulator (dimensions in mm) [18].

Finally, a commercial PD calibration device has been used to generate current pulses. Such a device is HVPD pC calibrator, which provides repeatable current pulses of specified charge from 1 pC up to 100 nC. Table 1 shows the calibrator specification.

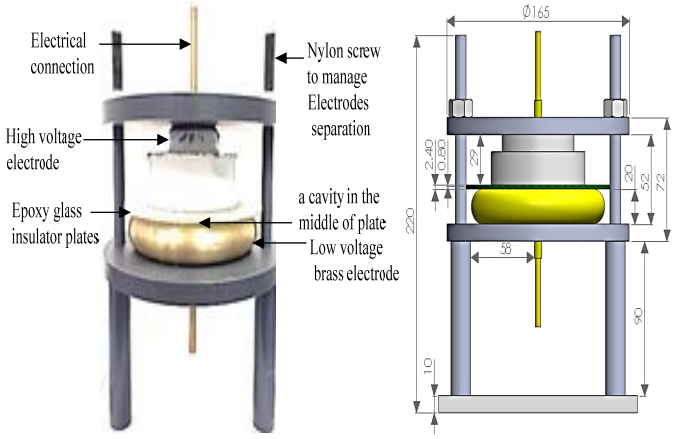

Figure 9. Epoxy dielectric internal PD emulator (dimensions in mm) [18].

Table 1. Calibrator specification.

pC output range	1pC to 100 nC
pC repetition rate	100 Hz, 120 Hz and 400 Hz
Battery Type	4 X AA / LR6
Battery life	Minimum 16 hours
Dimensions (mm)	180mm × 110mm × 49mm
Weight	0.56kg

3 EXPERIMENTAL RESULTS

3.1 RADIATED PD SIGNALS

A comparison between normalized signals captured by FSR and galvanic contact measurements using the floating-electrode emulator, the acrylic tube internal PD emulator, the acrylic tube internal PD emulator filled with transformer oil and finally the epoxy dielectric internal PD emulator is shown in Figure 10. The PD signals are compared under AC and DC voltages with the measurement system using the floating-electrode PD emulator. The PD event occurs by applying 6.2 kV DC or 15 kVrms AC voltage to the floating-electrode emulator. The PD inception voltage usually occurs at lower voltages under DC compared to AC voltage [21]. The internal PD emulators are measured using only AC voltage. The inception AC voltages for PD are: 20 kVrms for the acrylic tube PD emulator and the same for the acrylic tube emulator filled with transformer oil, and slightly lower at 18 kVrms for the epoxy dielectric internal PD emulator. The temporal decay of the signals in the two measurements seems to be similar. Bandwidth limitation is expected for the FSR measurement due to the electromagnetic radiation properties and the reception process. The bandwidth limitation is expected to be less severe in the case of galvanic contact measurement, resulting thus in less pronounced ringing. It is important to be noted that the bandwidth limitation is more due to the reactive characteristics of the PD source and the connecting cables

than due to the frequency response of the FSR receiving antenna [1, 22]. FSR and galvanic contact measurements were not synchronised in time during the experiments.

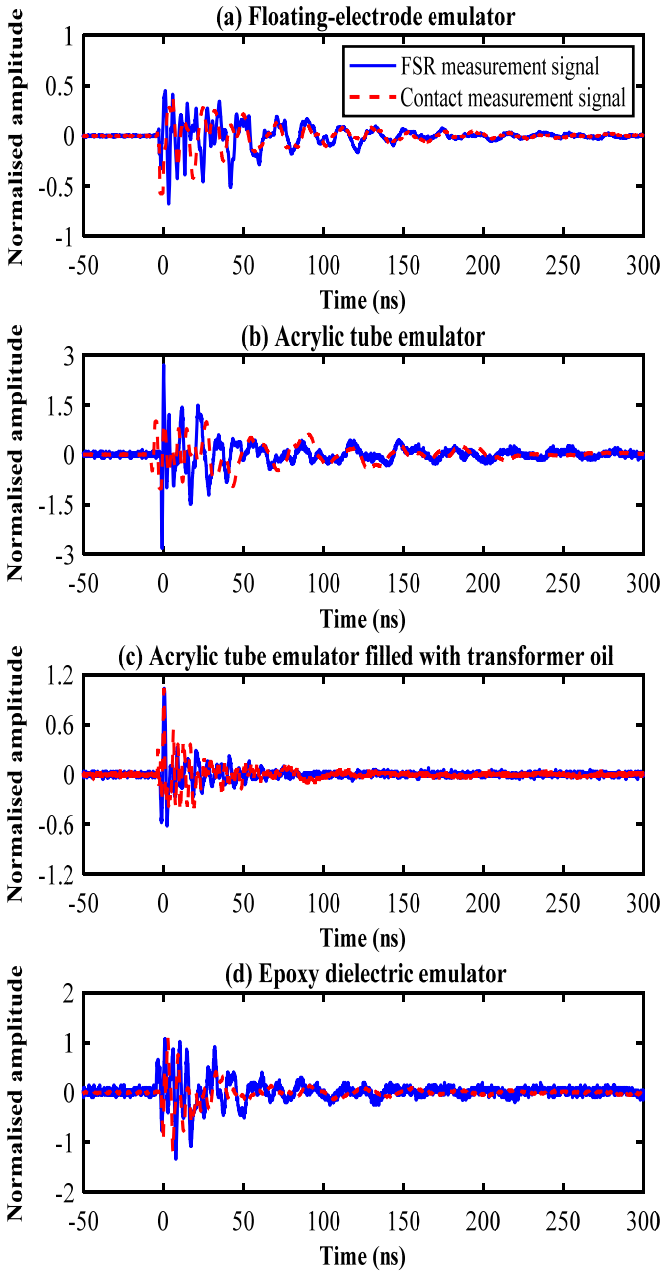

Figure 10. Comparison of normalized PD signals captured by FSR and galvanic contact measurements.

3.2 FSR PD MEASUREMENTS AND SIMULATIONS

A Gaussian current signal with a frequency spectrum in the VHF-UHF band has been used as excitation in the simulated PD sources. The Gaussian signal is as follows [18, 23, 24]:

$$i(t) = I_0 e^{\left(\frac{-(t-t_0)^2}{2\sigma^2}\right)} \quad (1)$$

where I_0 is the peak current, σ characterizes the pulse width and t_0 is the instant that corresponds to the pulse peak.

The electromagnetic wave propagation from the PD emulator model is simulated and recorded at a certain probe position. The radiated electric field is predicted by simulation at a distance of 2m for each of the emulators in response to the current pulse excitation. The simulation is implemented by using the time-domain solver of CST Microwave Studio (CST MWS).

The comparison between simulated and measured fields is exhibited in Figure 11. It seems that the simulated fields extracted from CST MWS are in good agreement with the measured ones for all the PD emulators. This gives confidence in the simulations, which may, therefore, be used to calculate the absolute PD intensity and apparent charge (in pC) and relate this to the radiated signal field strength at a particular distance from the PD source.

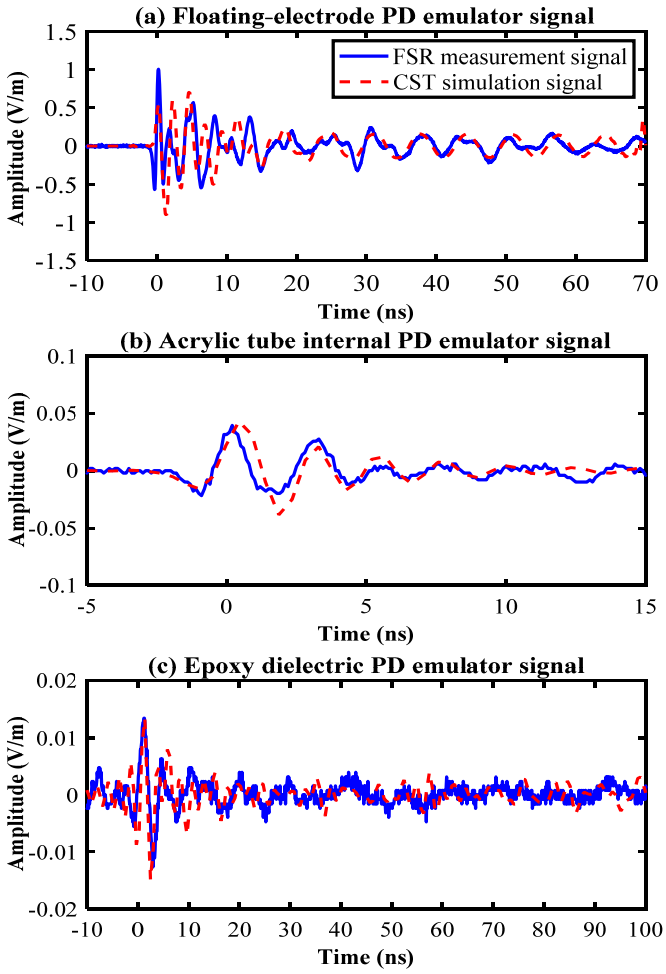

Figure 11. Comparison between measured and simulated PD electric field amplitudes [18].

3.3 FREQUENCY SPECTRA OF FSR AND GALVANIC CONTACT MEASUREMENTS

The frequency spectra are obtained by applying FFT to the time-domain signals. The normalized frequency spectra of the signals are compared in Figure 12. The energy resides almost entirely in the band of 50 MHz to 800 MHz with a preponderance of energy below 300 MHz. Although the spectra of FSR and galvanic contact measurements are not

identical, they have some similarities. The hypothesis that explains those similarities is that some of the diagnostic information about PD in a galvanic contact measurement remains in the radiometric measurement. This hypothesis is currently the subject of further investigation.

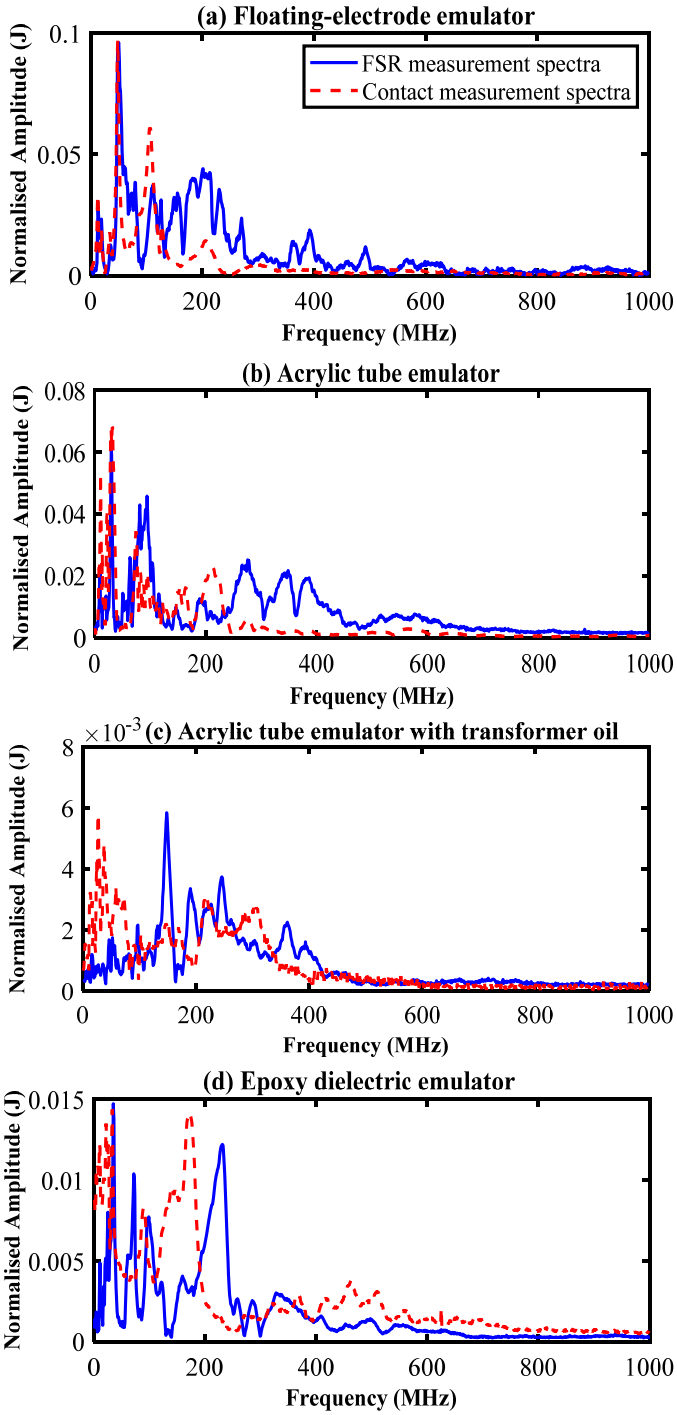

Figure 12. Comparison of normalized spectra captured by FSR and galvanic contact measurements.

3.4 PARTIAL DISCHARGE CALIBRATION

Classical PD measurements, as described in [13, 25], use a galvanic connection to conduct the PD current pulse (or a voltage pulse that is proportional to the current pulse) via a cable to the measurement instrument. If the measurement is sufficiently broadband for the pulse (which behaves as a baseband signal) then the pulse is easily, and unambiguously, integrated to find the apparent charge. However, if the pulse oscillates due to inductance and capacitance of the PD-source/measurement system combination, then a question arises about the accuracy of the apparent charge estimation. The integral from the start of the measured pulse to its first zero crossing (i.e., the first half-cycle integral) has been used as a measure of the apparent charge [26]. This metric has been investigated here by comparing it with a variety of known charges injected into the emulator using the HVPD calibrator. The accuracy of the first half-cycle method has been validated in practice by comparing to the known calibrator charge value when the calibrator is connected to the measurement setup. The measurement circuit applied to the floating electrode emulator is shown in Figure 13. Figure 14 shows the calculated (first half-cycle) charge against the charge injected by the calibration device [26]. Similar results have been obtained for all the PD emulators used in this study.

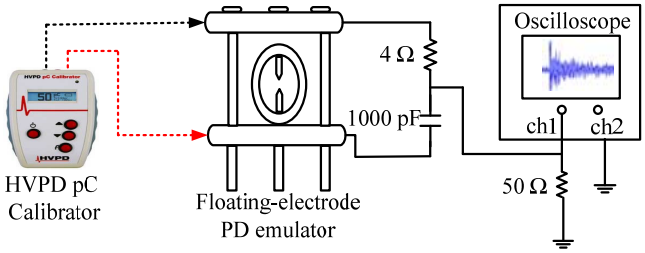

Figure 13. Measurement circuit for emulator calibration.

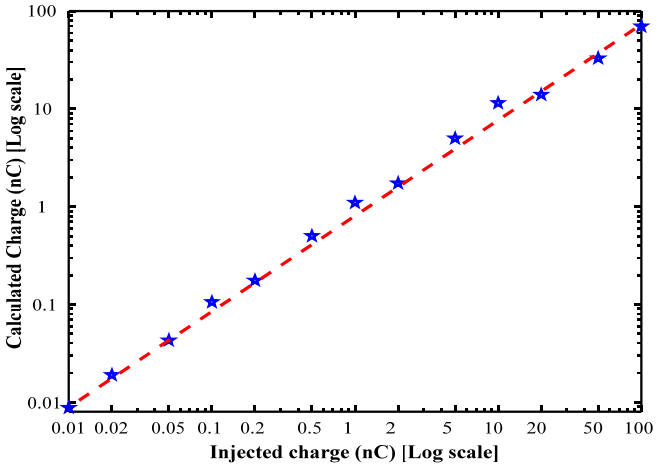

Figure 14. Half-cycle integrated current versus injected charge for the floating electrode PD emulator.

Figure 14 is a good evidence that the first half-cycle integral provides a useful estimate of the injected charge. By extension, we assume that the linear relationship will hold for the apparent charge.

Tables 2 to 4 show the variation with distance *d* of the received signal peak voltage, the calculated charge (from the first half-cycle integral of the received signal) and the calculated ERP for all PD emulators under AC applied voltages. AC voltage is used in all these experiments because

it produces more stable and repeatable results. The ERP of the emulator is estimated from the received field strength E by using the free-space propagation formula [27, 28], adapted for ERP values measured in dBm and distances measured in meters, as shown below:

$$E\,(dB\,\mu V/m) = 107 + ERP\,(dBm) - 20\log_{10} d\,(m) \qquad (2)$$

The received electric field strength is calculated by using the antenna factor of the biconical antenna, as given in Figure 6. It seems at least possible that an estimate of the ERP may represent a means of inferring absolute PD intensity (i.e., apparent charge) from a remote radiometric measurement such as those described in [29]. The apparent charge is estimated from the galvanic contact measurement method, while the FSR method is used for the estimation of ERP of the PD source. Figures 15-18 display the measured FSR peak voltage, the calculated field strength and the calculated ERP plotted versus distance d [26]. Effective radiated power should be independent of distance and discrepancies arise usually from reflections or near-field effects. The approximate value of ERP for the floating electrode PD emulator is approximately 25 to 27 dBm, however it is safer to assume a 'far-field' value of around 25 dBm. It is apparent that the peak ERP varies from 12.9 dBm to 12 dBm for an emulator without oil filling and from 7.7 dBm to 4.9 dBm for an emulator with oil filling. The average peak ERP is approximately 12 dBm in the case of emulator without oil filling and 7 dBm in the case of emulator with oil filling. The average peak ERP for epoxy dielectric internal PD emulator is around 1.4 dBm.

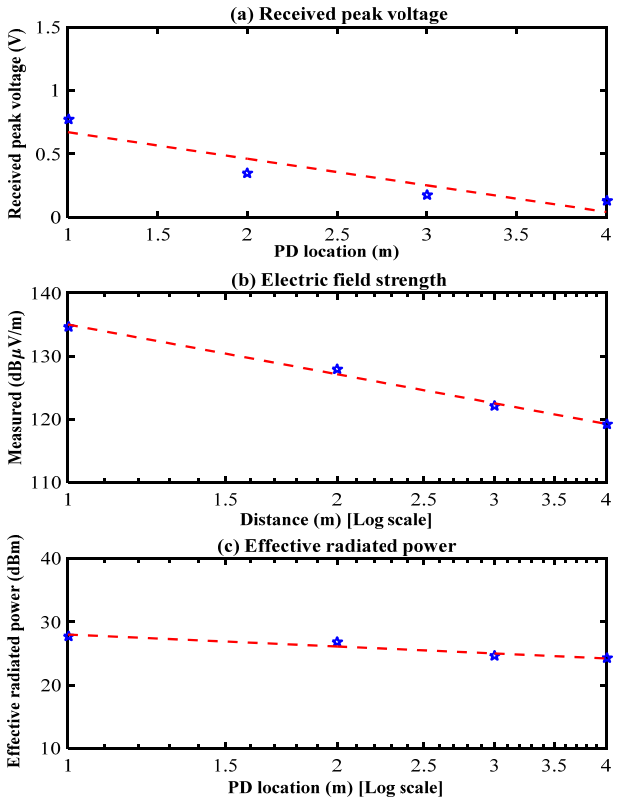

Figure 15. (a) Peak voltage, (b) Electric field strength, and (c) ERP as a function of antenna distance from the floating electrode PD emulator.

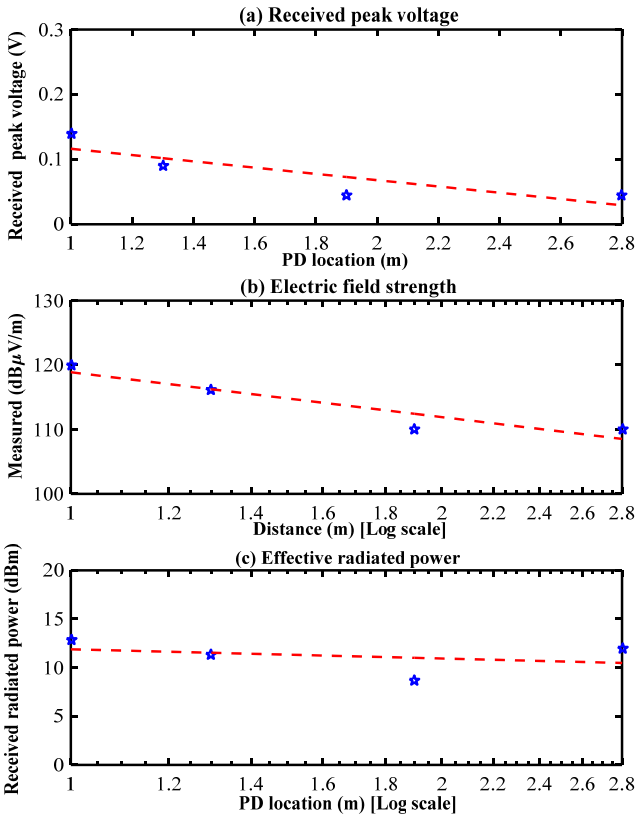

Figure 16. (a) Peak voltage, (b) Electric field strength, and (c) ERP as a function of antenna distance from the emulator (acrylic tube internal emulator without oil filling).

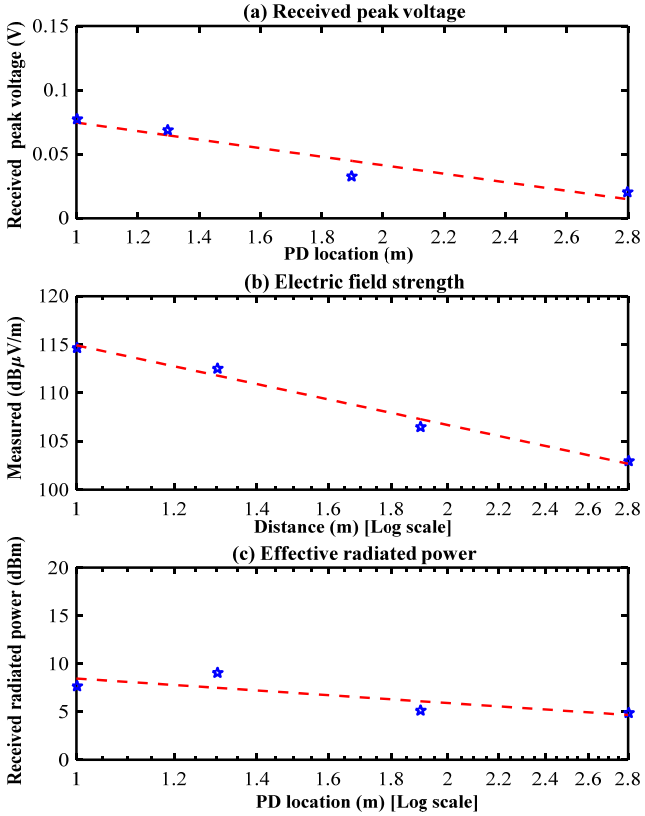

Figure 17. (a) Peak voltage, (b) Electric field strength, and (c) ERP as a function of antenna distance from the emulator (acrylic tube internal emulator with oil filling).

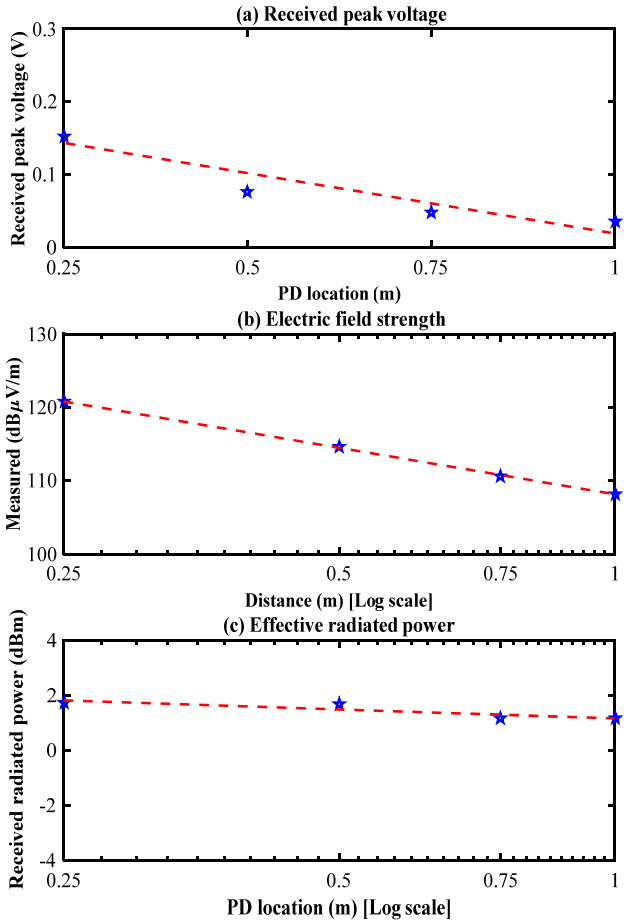

Figure 18. (a) Peak voltage, (b) Electric field strength, and (c) ERP as a function of antenna distance from the emulator (epoxy dielectric internal PD emulator).

The relationship between estimated apparent charge and estimated ERP for different PD emulator types is presented in Table 5. The apparent charge is calculated from galvanic measurements using the first half-cycle integration method and is given in the first row of Table 5. The estimated peak ERP in dBm is calculated from FSR measurements using the free-space propagation formula for short distances together with the measured antenna factor of the receiving antenna and is given in the second row of Table 5. The relationship between these two rows shows that the radiated power is proportional to the apparent charge of the PD, although the proportionality factor is not the same for all PD sources. Based on this fact, the apparent charges can be estimated from FSR measurements by taking into account the PD type (GIS, transformer, etc.) and the calibration curve of Figure 19, or a similar one. It seems that the radiated power of the floating electrode PD emulator is far greater than the radiated power of other types of emulators, and this by at least 13 dB. On the other hand, the epoxy dielectric internal PD emulator is radiating the least power. Finally, Figure 19 shows ERP in dBm versus apparent charge in nC, in an almost linear relationship, and suggests that the estimation of absolute PD intensity originating from HV insulation defects might be possible by using an FSR measurement alone.

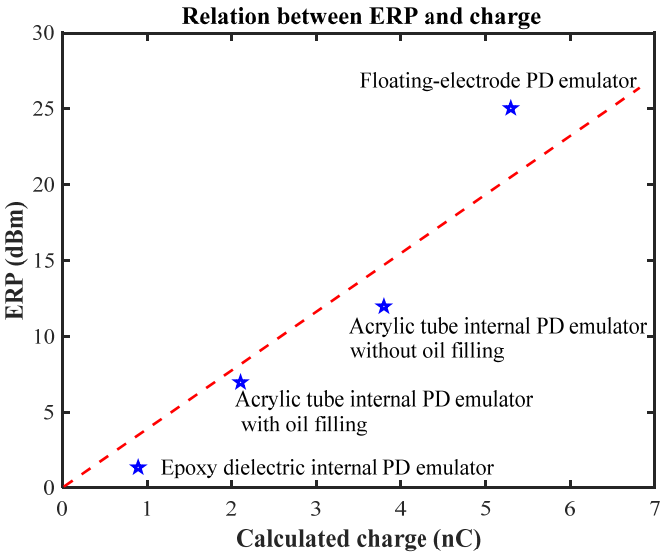

Figure 19. Determined ERP for different types of PD sources versus calculated charge.

Table 2. Simultaneous Measurements of FSR and Galvanic Measurements Using the Floating Electrode PD Emulator.

AC High-voltage source (kV)							
	Galvanic measurement	–	Galvanic mean peak voltage (V)	Galvanic mean peak voltage (dBμV)	Galvanic measurement standard deviation (V)	First half-cycle duration (ns)	Calculated charge (nC)
		–	6.57	136.3	2.29	6.9	5.3
15	FSR measurement	Antenna - emulator range (m)	FSR mean peak voltage (V)	FSR mean peak voltage (dBμV)	Peak electric field strength (dBμV/m)	Peak ERP (dBm)	Standard deviation (V)
		1	0.77	117.7	134.7	27.7	0.30
		2	0.35	110.8	127.9	26.8	0.09
		3	0.179	105.05	122.05	24.5	0.06
		4	0.129	102.2	119.2	24.2	0.03

Table 3. Concurrent measurements of FSR and galvanic measurements using the acrylic tube internal PD emulator with and without oil filling.

AC High-voltage source (kV)		–	Galvanic mean peak voltage (V)	Galvanic mean peak voltage (dBμV)	Galvanic measurement standard deviation (V)	First half-cycle duration (ns)	Calculated charge (nC)
	Galvanic contact measurement			Without oil filling			
		–	3.91	131.8	1.98	10.4	3.8
				Oil filling			
		–	2.76	128.8	1.28	4.7	2.1
20		Antenna - emulator range (m)	FSR mean peak voltage (V)	FSR mean peak voltage (dBμV)	Peak electric field strength (dBμV/m)	Peak ERP (dBm)	Standard deviation (V)
	FSR measurement			Without oil filling			
		1	0.14	102.9	119.9	12.9	0.06
		1.30	0.09	99.08	116.08	11.3	0.03
		1.90	0.04	93.06	110.06	8.63	0.01
		2.80	0.04	93.06	110.06	12.00	0.01
				Oil filling			
		1	0.07	97.7	114.7	7.7	0.02
		1.30	0.06	95.5	112.5	9.0	0.03
		1.90	0.03	89.5	106.5	5.1	0.01
		2.80	0.02	86.0	103.0	4.9	0.01

Table 4. Simultaneous measurements of FSR and galvanic pulses using the epoxy dielectric internal PD emulator.

AC High - voltage source (kV)	Galvanic measurement	–	Galvanic mean peak voltage (V)	Galvanic mean peak voltage (dBμV)	Galvanic measurement standard deviation (V)	First half-cycle duration (ns)	Calculated charge (nC)
		–	1.66	124.4	0.82	4.8	0.9
18	FSR measurement	Antenna emulator range (m)	FSR mean peak voltage (V)	FSR mean peak voltage (dBμV)	Peak electric field strength (dBμV/m)	Peak ERP (dBm)	Standard deviation (V)
		0.25	0.153	103.7	120.7	1.73	0.060
		0.50	0.076	97.7	114.7	1.70	0.029
		0.75	0.048	93.6	110.6	1.17	0.018
		1.00	0.036	91.1	108.1	1.15	0.016

Table 5. Relationship between Calculated Charge and ERP of PD Emulators.

PD emulator	Floating-electrode PD emulator	Acrylic tube internal PD emulator without oil filling	Acrylic tube internal PD emulator with oil filling	Epoxy dielectric internal PD emulator
Calculated charge (nC)	5.3	3.8	2.1	0.9
Estimated peak ERP (dBm)	25	12	7	1.4

4 CONCLUSION

Evidence has been presented that diagnostic information in galvanic PD measurements originating from HV insulation defects may still be present in FSR measurements. Such diagnostic information is used to calculate the absolute PD intensity if the distance from the PD source is known and ERP can reliably be estimated. Since radiometric location of PD sources is possible with multiple radiometric sensors, a calculation of the absolute PD intensity from a radiometric measurement alone is certainly possible.

ACKNOWLEDGMENT

The authors would like to acknowledge the Engineering and Physical Sciences Research Council for their support of this work under grant EP/J015873/1.

REFERENCES

[1] A. Jaber, P. Lazaridis, Y Zhang, D Upton, H Ahmed, U Khan, B Saeed, P Mather, M F Q Vieira, R Atkinson, M Judd, and I A Glover, "Comparison of contact measurement and free-space radiation measurement of partial discharge signals," 21st Int'l. Conf., Automation and Computing (ICAC), Glasgow, UK, pp. 1-4, 2015.

[2] D. A. Genutis, "Using Partial Discharge Surveys to Increase Electrical Reliability," Annual Technical Conf. Communications and Metering-Neta World, USA, pp. 69-73, 2002.

[3] D. A. Genutis, "Partial Discharge Monitoring of Medium-Voltage Switchgear," Neta World, USA, pp. 1, 2010.

[4] S. Grubic, J. M. Aller, B. Lu, and T. G. Habetler, "A survey on testing and monitoring methods for stator insulation systems of low-voltage induction machines focusing on turn insulation problems," IEEE Trans. Industrial Electronics, Vol. 55, pp. 4127-4136, 2008.

[5] D. A. Genutis, "On-Line Shielded Cable Partial Discharge Locating — An Overview," Neta World, USA, pp. 1-3, 2006.

[6] D. A. Genutis, "Partial Discharge Testing of Rotating Apparatus," Neta World, USA, pp. 1-2, 2008.

[7] M. Aruna, V. Pattanshetti, K. N. Ravi, and N. Vasudev, "Insulation System in Energy Sector: The Benefits of Polymer Composites," Indian J. Appl. Research, Vol. 1, Issue. 2, pp. 44-47, 2011.

[8] D. A. Genutis, "Electrical Equipment Condition Assessment Using On-Line Solid Insulation Sampling," Neta World, USA, pp. 1-5, 2006.

[9] E. Iliana, J. Philip, and I. A. Glover, "RF-Based Partial Discharge Early Warning System for Air-Insulated Substation," IEEE Trans. Power Delivery, vol. 24, pp. 20-29, 2009.

[10] Q. Zhang, C. Li, S. Zheng, H. Yin, Y. Kan, and J. Xiong, "Remote detecting and locating partial discharge in bushings by using wideband RF antenna array," IEEE Trans. Dielectr. Electr. Insul., Vol. 23, pp. 3575-3583, 2016.

[11] A. Reid, M. Judd, B. Stewart, D. Hepburn, and R. Fouracre, "Identification of multiple defects in solid insulation using combined RF and IEC60270 measurement," IEEE Int'l. Conf. Solid Dielectrics, (ICSD), pp. 585-588, 2007.

[12] S. Coenen, S. Tenbohlen, S. Markalous, and T. Strehl, "Sensitivity of UHF PD measurements in power transformers," IEEE Trans. Dielectr. Electr. Insul., Vol. 15, pp. 1553-1558, 2008.

[13] I. E. Commission, IEC 60270, " High-voltage Test Techniques: Partial Discharge Measurements," International Electrotochnical Commission, India, pp. 1-51, 2000.

[14] E. Lemke, S. Berlijn, E. Gulski, M. Muhr, E. Pultrum, T. Strehl, et al., "Guide for partial discharge measurements in compliance to IEC 60270," CIGRE Technical Bochure, Vol. 366, 2008.

[15] A. J. Reid, M. D. Judd, R. A. Fouracre, and D. M. Hepburn. Simultaneous measurement of partial discharges using IEC60270 and radio frequency techniques. IEEE Trans. Dielectr. Electr. Insul., Vol. 18, No. 2, pp. 444-445, 2011.

[16] A. Jaber, P. Lazaridis, B. Saeed, Y. Zhang, U. Khan, D. Upton, H. Ahmed, P. Mather, M. F. Q. Vieira, R. Atkinson, M. Judd, and I. A. Glover, "Comparative study of Partial Discharge Emulators for the Calibration of Free-Space Radiometric Measurements," 22nd Int'l. Conf. Automation and Computing (ICAC), Colchester, UK, 2016, pp. 313-316, 2016.

[17] B. Hampton, "UHF diagnostics for gas insulated substations," 11th Int'l. Sympos. High Voltage Eng., pp. 6-16, 1999.

[18] A. Jaber, P. Lazaridis, B. Saeed, Y. Zhang, U. Khan, D. Upton, H. Ahmed, P. Mather, M. F. Q. Vieira, R. Atkinson, M. Judd, and I. A. Glover, "Validation of Partial Discharge Emulators Simulation using Free-Space Radiometric Measurements," Int'l. Conf. Students Appl. Eng. (ISCAE), Newcastle, UK, pp. 475-478, 2016.

[19] J. M. R. de Souza Neto, E. C. T. de Macedo, J. S. da Rocha Neto, E. G. Da Costa, S. A. Bhatti, and I. A. Glover.,"Partial Discharge Location using Unsynchronized Radiometer Network for Condition Monitoring in HV Substations-A Proposed Approach," Conf. Series, Proposed Approach", J. Phys., vol. 364, no. 1, p. 012053. IOP Publishing, 2012.

[20] M. G. Niasar, N. Taylor, P. Janus, et al., "Partial discharges in a cavity embedded in oil-impregnated paper: effect of electrical and thermal aging," IEEE Trans. Dielectr. Electr. Insul., Vol. 22, pp. 1071-1079, 2015.

[21] R. Sarathi, A. Reid, and M. D. Judd, "Partial discharge study in transformer oil due to particle movement under DC voltage using the UHF technique," Electric Power Systems Research, Vol. 78, pp. 1819-1825, 2008.

[22] A. Jaber, P. Lazaridis, B. Saeed, Y. Zhang, U. Khan, D. Upton, H. Ahmed, P. Mather, M. F. Q. Vieira, R. Atkinson, M. Judd, and I. A. Glover "Frequency Spectrum Analysis of Radiated Partial Discharge Signals," IET EUROEM Conf. (European Electromagnetics Symposium), London, UK, pp. 1-2, 2016.

[23] H. Karami, G. B. Gharehpetian, and M. S. A. Hejazi, "Oil Permittivity Effect on PD Source Allocation Through Three-dimensional Simulation," Int'l. Power System Conf., Tehran- Iran, 2013, pp. 1-5, 2013.

[24] M. Zanjani, A. Akbari, N. Shirdel, E. Gockenbach, and H. Borsi, "Investigating partial discharge UHF electromagnetic waves propagation in transformers using FDTD technique and 3D simulation, IEEE Int'l. Conf. Condition Monitoring and Diagnosis, Bali, Indonesia, pp. 497-500, 2012.

[25] A. Cavallini, G. C. Montanari, and M. Tozzi, "PD apparent charge estimation and calibration: A critical review," IEEE Trans. Dielectr. Electr. Insul., Vol. 17, 2010.

[26] A. Jaber, P. Lazaridis, Y. Zhang, B. Saeed, U. Khan, D. Upton, H. Ahmed, P. Mather, M. F. Q Vieira, R Atkinson, M. Judd, and I. A. Glover, "Assessment of absolute partial discharge intensity from a free-space radiometric measurement," URSI Asia-Pacific Radio Science Conf. (URSI AP-RASC), Seoul, Korea, pp. 1011-1014, 2016.

[27] C. Haslett, *Essentials of Radio Wave Propagation,* UK, Cambridge University Press, 2008.

[28] M. Hata, "Empirical formula for propagation loss in land mobile radio services," IEEE Trans. Vehicular Technology, Vol. 29, pp. 317-325, 1980.

[29] Y. Zhang, D. Upton, A. Jaber, H. Ahmed, B. Saeed, P. Mather, P. Lazaridis, A. Mopty, C. Tachtatzis, R. Atkinson, M. Judd, M F Q Vieira, and I A Glover, "Radiometric wireless sensor network monitoring of partial discharge sources in electrical substations," Hindawi, Int'l. J. Distributed Sensor Networks, Vol. 2015, pp. 1-9, 2015.

Adel A. Jaber was born in Tripoli, Libya in 1973. He received the higher diploma degree in electricity from the higher institute, Malta in 1995, the M.Sc. degree in control and electronics from the Teesside University, Middlesbrough, United Kingdom, in 2011. He has completed his a PhD degree from the Department of Engineering and Technology, University of Huddersfield, United Kingdom. His research is focused on absolute calibration of radiometric partial discharge sensors for insulation condition monitoring in electrical substations.

Pavlos I. Lazaridis (M'13-SM'15) received the BSc degree in electrical engineering from Aristotle University of Thessaloniki, Greece, in 1990, the MSc in electronics from Université Pierre & Marie Curie, Paris 6, France in 1992 and the PhD from ENST Paris and Paris, in 1996. From 1991 to 1996, he was involved with research on semiconductor lasers and wave propagation for France Télécom and teaching at ENST Paris. In 1997, he became Head of the Antennas and Propagation Laboratory, TDF- C2R Metz (Télédiffusion de France/France Télécom Research Center). From 1998 to 2002 he was senior Examiner at the European Patent Office (EPO), Den Haag, the Netherlands. From 2002 to 2014 he was involved with teaching and research at the ATEI of Thessaloniki, Greece and Brunel University West London. He is currently a Reader in Electronic and Electrical Engineering at the University of Huddersfield, United Kingdom, member of the IET, and a Fellow of the Higher Education Academy.

Mohamamd Moradzadeh is a Senior Lecturer in Electrical Power Engineering in the Department of Engineering & Technology at the University of Huddersfield, UK. He received his PhD degree from Ghent University, Ghent, Belgium, in 2012, and the MSC degree from K.N. Toosi University of Technology, Tehran, Iran, in 2007, both in electrical power engineering. He worked as a Postdoctoral Fellow in Ghent University during 2013–2015, and then joined the University of Windsor, Windsor, ON, Canada as a Program Development Administrator for an academic year. His main research interests are in the area of smart grids, integration of renewables and provision of ancillary services by wind turbines.

Ian A. Glover is a Radio Scientist and Wireless Communications Engineer. He is currently Professor of Radio Science & Wireless System Engineering, and Head of the Department of Engineering and Technology, at the University of Huddersfield in the UK. He is also Visiting Professor of Radio Science at the Universidade Federal de Campina Grande in Brazil. He has previously held senior academic posts at the Universities of Strathclyde, Bath and Bradford. Ian's principal current research interest is in the application of radiometric and wireless communication methods to insulation condition monitoring and asset management of high-voltage plant in the future smart grid. His other interests are in classical radio propagation for applications ranging from satellite communication, terrestrial microwave radio relay, mobile communications, radar and wireless sensor networks. He is the Chair of the UK Panel of the International Union of Radio Science (URSI) and is a past Associate Editor of the Radio Science Bulletin. He is the author, with Peter Grant, of Digital Communications (1998, 2004, 2008) published by Pearson and the editor (with Peter Shepherd and Stephen Pennock) of Microwave Devices, Circuits and Subsystems for Communications Engineering (2005) published by Wiley. Ian Glover is a member of the IET, IEEE and IoP, and is a Fellow of the Academy of Higher Education.

Zaharias D. Zaharis (M'13-SM'15) received the B.Sc. degree in Physics in 1987, the M.Sc. degree in Electronics in 1994, and the Ph.D. degree in 2000 from Aristotle University of Thessaloniki. Also, in 2011 he obtained the Diploma degree in Electrical and Computer Engineering from the same university. From 2002 to 2013, he has been working in the administration of the telecommunications network of Aristotle University of Thessaloniki. Since 2013, he is with the Department of Electrical and Computer Engineering, Aristotle University of Thessaloniki. His research interests include design and optimization of antennas and microwave circuits, mobile communications, radio-wave propagation, RF measurements, evolutionary optimization, neural networks, and signal processing. Dr. Zaharis is a member of the Technical Chamber of Greece.

Maria de Fatima Queiroz Vieira is a full professor in Electrical Engineering at UFCG, in Brazil and a Research Fellow in the Engineering and Technology Department at the University of Huddersfield in the UK. She graduated in electrical engineering at UFPB, in Brazil (1981); and got her PhD in electrical engineering at Bradford University in the UK (1986). Her research field is Human Systems Interaction Ergonomics with focus on mitigating the human error in Automated System in Industrial environments, such as the electric systems network installations. Along her career, she has collaborated with institutions in France (Universities of Marseille and Aix en Provence) and in the UK (Universities of Strathclyde and Huddersfield). She has been the head of the Man-Machine Interface Laboratory (LIHM) at UFCG since 1986.

Martin D. Judd (M'02-SM'04) is Technical Director of High Frequency Diagnostics Ltd, based in Glasgow, Scotland. He graduated from the University of Hull in 1985 with a first class (Hons) degree in Electronic Engineering, after which he gained 8 years of industrial experience, first with Marconi Electronic Devices and then with EEV Ltd. Martin received his PhD from the University of Strathclyde in 1996 for research into the excitation of UHF signals by partial discharges in gas insulated switchgear. He has worked extensively on UHF partial discharge location techniques for power transformers and was latterly Professor of High Voltage Technologies at the University of Strathclyde, where he managed the High Voltage Research Laboratory. In 2014 he founded High Frequency Diagnostics, a specialist consultancy business that works in partnership with companies developing new electromagnetic wave sensor technologies and applications.

Robert C Atkinson is a Senior Lecturer in the Department of Electronic and Electrical Engineering, University of Strathclyde. He has applied a range of signal processing and machine learning algorithms to a range of fields as diverse as: radiolocation of partial discharge, intrusion detection systems, 4G handover optimization, game theory applied to radio access network selection, prognostics for gearboxes, condition-based maintenance of water pumps, internet of things, smart cities, smart buildings, and image analysis for pharmaceutical crystals. He is the author of over 80 scientific papers, published in internationally recognized conferences and journals. He is a Member of the IET and a Senior Member of the IEEE.